Unconventional MBE strategies from computer simulations for optimized growth conditions

S. Schinzer*
Institut für Theoretische Physik, TP III, Universität Würzburg, Am Hubland, D-97074 Würzburg, Germany

M. Sokolowski
Institut für Experimentelle Physik, EP II, Universität Würzburg, Am Hubland, D-97074 Würzburg, Germany

M. Biehl and W. Kinzel
Institut für Theoretische Physik, TP III, Universität Würzburg, Am Hubland, D-97074 Würzburg, Germany
(Received 21 December 1998)

We investigate the influence of step-edge diffusion (SED) and desorption on molecular-beam epitaxy (MBE) using kinetic Monte Carlo simulations of the solid-on-solid model. Based on these investigations we propose two strategies to optimize MBE growth. The strategies are applicable in different growth regimes: During layer-by-layer growth one can exploit the presence of desorption in order to achieve smooth surfaces. By additional short high flux pulses of particles one can increase the growth rate and assist layer-by-layer growth. If, however, mounds are formed (non-layer-by-layer growth), the SED can be used to control size and shape of the three-dimensional structures. By controlled reduction of the flux with time we achieve a fast coarsening together with smooth step edges. [S0163-1829(99)04727-X]

I. INTRODUCTION

The growth of high-quality compound semiconductors is of great technological importance.[1] Despite the longstanding tradition of molecular-beam epitaxy (MBE), it is still a challenging task to improve the growth of high-quality thin films and well-defined interfaces. In order to optimize MBE growth, a detailed knowledge of the relation between microscopic processes and macroscopic properties is very important. Computer simulations are an ideal tool to access this relation between atomistic processes and epitaxial growth. In addition, different growth strategies can be easily implemented and tested in a fast and cheap way.[2,3]

In this paper we will investigate the macroscopic effects of two distinct microscopic mechanisms. The term *microscopic* refers to processes on the atomic scale: e.g., a single diffusion step of an adatom or desorption of an atom. These processes are the ingredients to the computer model used in this paper. This is contrasted to the term *macroscopic* for effects which are typically measurable in experiments: e.g., the overall mass desorption, as can be monitored by the partial pressure,[4] the form, and the distribution of three-dimensional structures accessible by scanning tunneling microscopy,[5] or the growth rate as determined by electron-diffraction oscillations.[6] The computer simulations employed here are ideally suited to bridge the gap between such macroscopic effects and their underlying microscopic processes, since both scales are accessible.

Several strategies have been proposed in the literature to optimize MBE growth: In particular, layer-by-layer growth is most desirable in order to achieve high-quality thin films.[2,3] However, quite often a transition to non-layer-by-layer growth is observed where three-dimensional (3D) structures such as mounds or pyramids appear. In *conventional* MBE,[7] the time $t_\times$ until this growth mode crosses over to 3D growth has been shown to vary with $Ft_\times \approx (D/F)^\delta$,[8] where F stands for the flux and D for the diffusion constant of adatoms. Without desorption, Ehrlich-Schwoebel barriers and step edge diffusion (SED) $\delta = 2/3$ has been observed for epitaxial growth.[9] For metals, several methods have been proposed and tested to achieve and maintain layer-by-layer growth. For instance, it has been shown that pulsing the deposition rate or pulsing the temperature leads to a prolonged layer-by-layer regime.[2] Recently, it has been proposed that pulsed glancing-angle sputtering can even lead to ''layer-by-layer growth forever.''[3] All these concepts can so far be understood in terms of a typical diffusion length or an enhanced interlayer diffusion at step edges.

In this paper we will propose strategies which exploit other specific microscopic processes, namely, desorption[10] and SED.[11,12] As far as we know, no attempt has been made to exploit these processes in order to achieve improved growth. Some preliminary results of our investigation were published in Ref. 13, and in this paper we describe the investigation in full detail.

In Sec. II we introduce the solid-on-solid (SOS) model and the microscopic processes. In our computer experiments we first investigated the temperature dependence of the overall growth rate in the layer-by-layer regime (Sec. III). We are able to correlate this macroscopic property to the microscopic dynamics of the computer model. This allows us to propose a strategy for layer-by-layer growth. If, however, the growth of three-dimensional structures occurs, another strategy is applicable. Using a simplified model of growth we have recently shown that SED plays a crucial role in this regime.[14,15] These findings allow us to propose an optimized way for the growth of 3D structures in Sec. IV. Concluding remarks concerning the experimental realisation and a summary will be given in Sec. V.

II. COMPUTATIONAL MODEL

Lattice models with the SOS restriction have been proved to be a useful tool to study surface morphology.[16,17] The

model has a long history for the study of the surface roughness transition.[18] Gilmer and Bennema were the first (to our knowledge) to include surface diffusion.[19] Since then it has been intensively used to study epitaxial growth.[20,21]

Here we use its most simple form, where only one kind of particle and a simple cubic lattice is considered. The particles represent single atoms when a comparison with a simple cubic metal is made. However, even compound semiconductors can be modeled, as long as kinetic features are investigated only. That is, in Ref. 22 the reflection high-energy electron-diffraction oscillations of GaAs(001) during growth have been quantitatively reproduced.

In our simulations we use the Maksym algorithm of Ref. 23. At each time step a Monte Carlo move is carried out. The way the event is selected makes it superior to conventional Monte Carlo techniques (the algorithm uses partly a binary search in the array of possible events). We have used a system of 300×300 lattice sites, if not stated otherwise.

Besides the SOS restriction, further simplifications are due to the particular choice of possible events labeled i and the parametrization of the corresponding rates Γ_i. We allow jumps to the four nearest-neighbor sites (diffusion on a flat surface, attachment and detachment from steps, etc.) and desorption. The rates do only depend on the four nearest-neighbor sites as will be described below. We describe all these processes as Arrhenius activated,

$$\Gamma_i = \nu_i \exp\left(-\frac{E_i}{k_B T}\right), \tag{1}$$

as predicted by several theories.[24]

One quite often assumes vibration frequencies ν_i of the order of Debye frequencies, i.e., 10^{12}–10^{14} s^{-1}. Indeed, in sublimation experiments of CdTe(001), 10^{14} s^{-1} has been observed;[4,25] vibrational frequencies for diffusion are often of the order of 10^{12} s^{-1} [measurements for metals,[26] calculations for GaAs(001),[27,28] or simulations and calculations for Si(001)[29,30]]. Hence it is reasonable to assume that the diffusion as well as the desorption rates of our model share one common prefactor $\nu_i=\nu_0=10^{12}$ s^{-1} which allows one to keep the number of parameters small.

The activation energy for the different microscopic processes are parametrized as follows: a diffusion jump of a free adatom has to overcome a barrier E_B, each next in-plane neighbor adds an energy E_N. The rate of diffusion jumps which keep the height of the particle unchanged thus becomes $\nu_0\exp[-(E_B+nE_N)/k_BT]$, where n represents the number of next in-plane neighbors. Note that the overall rate for diffusion on a flat surface is four times this jump rate due to the four possible directions. Hence the diffusion constant becomes $D=\nu_0\exp(-E_B/k_BT)$.[31] Since we measure all length scales in units of the lattice constant a we have neglected the term a^2 in D. At step edges an additional Ehrlich-Schwoebel barrier E_S is considered.[32,33] However, this barrier is not added for particles on top of an elongated island of only one lattice constant width.[34] The desorption barrier is E_D. Again, each next in-plane neighbor contributes E_N.

The deposition of particles occurs with a rate F measured in monolayers per second (ML/s). During deposition we consider another process which is not Arrhenius activated. After a deposition site is chosen randomly, we allow the particle to relax to a lower neighboring site. Here we consider only relaxation to nearest-neighbor sites. Such *transient diffusion* or *downward funneling* has been observed in molecular dynamics of simple Lennard-Jones systems,[35,36] and has been related to the reentrant layer-by-layer growth at very low temperatures.[37] In addition it has been shown to play a crucial role for slope selection in mound morphology.[14]

We will concentrate on one set of parameters, namely, $E_B=0.9$ eV, $E_N=0.25$ eV, $E_S=0.1$ eV, and $E_D=1.1$ eV. This particular choice of parameters reproduces some features of CdTe(001) during sublimation[38,39] and annealing. However, we would like to stress that the findings of our present work are of more general relevance, independent of the specific choice of the energetic parameters.

III. REEVAPORATION DURING LAYER-BY-LAYER GROWTH AND THE FLUSH TECHNIQUE

For clarity we will distinguish several processes of desorption. The term *desorption* will be explicitly used to describe the atomistic process: the desorption of a single atom. *Sublimation* is reserved to describe the evaporation of a surface when left in (perfect) vacuum. *Reevaporation* or more precisely *reevaporation during growth* will describe the overall desorption rate mostly due to the desorption of freshly deposited particles during growth.

For two of the most important compound semiconductors a decrease of the MBE growth rate with increasing temperature was observed [CdTe(001)[6,40,25] and GaAs[41,42]]. For CdTe(001) the reevaporation rate was found to follow an Arrhenius rate with considerably lower values of the activation energy of 0.14–0.30 eV compared to sublimation (1.55 eV or 1.9 eV,[39] respectively). A tempting explanation is to ascribe this low energy to the existence of a physisorbed precursor.[25] However, studies of the sublimation with computer simulation[38] as well as experiments for CdTe(001) (Ref. 39) showed a strong influence of the morphology. In Ref. 38 we already concluded that in MBE, one should expect desorption rates other than those measured by sublimation. Independently Pimpinelli and Peyla also showed that a physisorbed precursor is not necessary to explain the observed low energies using kinetic Monte Carlo simulations as well as simple scaling arguments.[43,44]

In Fig. 1, the diamonds represent the reevaporation which we derived from the difference between the applied flux ($F=1$ ML/s) and the measured growth rate (i.e., the reached height/simulated time). The data points for $F=4$ ML/s ($\bigcirc$) show that the effective energy is independent of the applied flux. The triangles correspond to the sublimation, i.e., the evaporation rate without application of an external flux ($F=0$ ML/s).[38] Both processes are found to be Arrhenius activated, though, with strikingly different effective energies. The reevaporation rate during growth corresponds to an activation energy of approximately 0.90 eV which is even lower than the microscopic desorption energy of $E_D=1.1$ eV. At high temperatures the reevaporation rate saturates and equals the flux of impinging particles. Conversely, the sublimation energy of approximately 1.73 eV is considerably higher.[45]

The relation of the sublimation energy to the microscopic parameters was shown to be approximated by E_{sub}

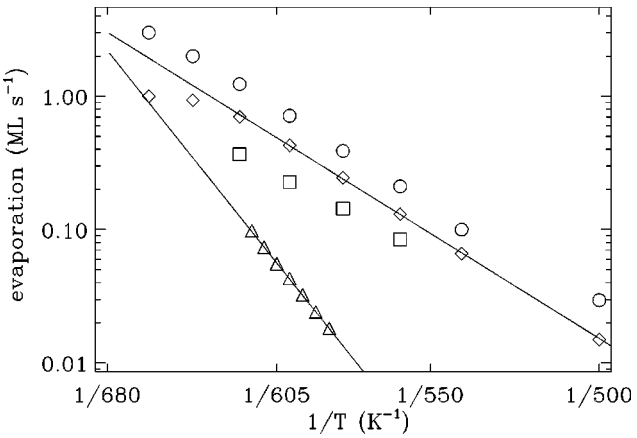

FIG. 1. Reevaporation rate during growth with $F=1$ ML/s ($\diamond$), $F=4$ ML/s ($\circ$), and sublimation rate $\times 10$ at $F=0$ ML/s ($\triangle$). In addition, we show the reevaporation rate using the proposed flush technique ($\square$) with a mean flux of 1 ML/s consisting of a constant flux of 0.77 ML/s plus an additional pulse of 0.23 ML during 0.003 s at the beginning of each second.

$\approx 0.61E_B + 0.35E_D + 2.85E_N + 0.44E_S$.[38] To derive this relation we varied all microscopic energy parameters independently. Applying the same microscopic analysis to the reevaporation during growth of this model, we obtain

$$E_{\mathrm{re}} \approx -0.31E_B + 0.94E_D + 0.51E_N - 0.03E_S. \qquad (2)$$

As an example for this microscopic analysis, Fig. 2 shows the measured influence of the diffusion barrier E_B and of the desorption barrier E_D to the reevaporation rate. We applied a flux of $F=4$ ML/s. Since the measured reevaporation rate is much lower (less than 1 ML/s), we can be sure to have no saturation effects. Note the opposite sign of the two contributions. The slope measures the prefactor in the above expression of E_{re} [Eq. (2)].

We want to mention that this result does not agree with the scaling relation obtained by Pimpinelli and Peyla.[43] However, at lower temperatures (not shown) we observe a crossover to their result with a critical nucleus size of $i^*=1$. The crossover itself can be seen at the data point for $F=4$ ML/s at 500 K which lies above the value of about 0.2 ML/s which is extrapolated at 500 K from data points at higher temperatures. A detailed investigation of the validity regime of our result and the relation to the results obtained by Pimpinelli and Peyla will be postponed to a future work.

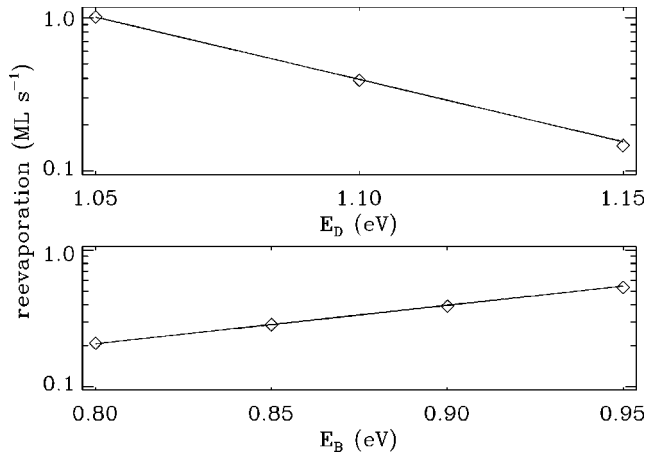

FIG. 2. Variation of the reevaporation rate during growth as a function of the desorption barrier E_D (upper) and diffusion barrier E_B (lower curve). The slope gives the contribution to the effective energy. The simulations were carried out at $T=560$ K, with $F=4$ ML/s.

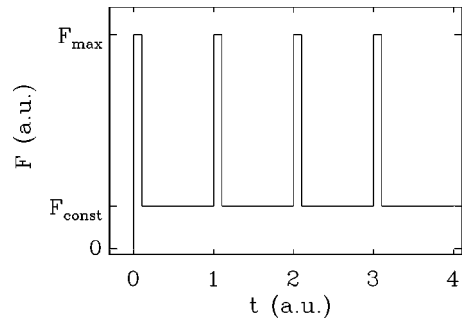

FIG. 3. Schematic variation of the flux using the flush technique.

Besides the different weightings in E_{re} and E_{sub}, the striking difference (at high as well as low temperatures) is the negative contribution of the diffusion barrier E_B to E_{re}. This result seems to be of general validity,[43] and can be explained in the following way: Even though the island distance is influenced by E_B, the dominant effect of higher diffusion barriers seems to be the reduction of the diffusion length of the adatoms. Consequently, particles have a higher probability for desorption before they stick to an island.

This result suggests a strategy to obtain high-quality (layer-by-layer) growth together with high growth rates. Short flushes of particles at the beginning of each monolayer would result in a great density of islands. Afterwards with a low flux the particles probably hit islands to stick to which will result in a low overall reevaporation rate. The proposed procedure (flush-mode) is drawn schematically in Fig. 3.

Figure 1 shows that the reevaporation rate indeed reduces by a factor of about 2 when applying this strategy. The mean flux was 1 ML/s as for the conventional growth simulations. The profile of the flux was composed as follows: At intervals of 1 s we deposited a total amount of 0.23 ML within 0.003 s (see Fig. 3). Afterwards a constant flux of 0.77 ML/s was applied. According to the decrease of evaporation the growth rate increases. The gain is highest at high temperatures (at 620 K the growth rate is doubled) since there the evaporation rate becomes comparable to the applied flux.

In addition to higher growth rates, layer-by-layer growth is assisted by the flush mode. In Fig. 4 we compare three different techniques/models of growth: (A) conventional growth with $F=1$ ML/s and allowed desorption; (B) a flush mode with $F_{\mathrm{const}}=1$ ML/s and an additional 0.30 ML in 0.003 s each second and allowed desorption; and (C) a flush mode without desorption ($E_D=\infty$), $F_{\mathrm{const}}=0.77$ ML/s, and an additional 0.23 ML during 0.003 s each second. The different fluxes in (B) and (C) are chosen in order to achieve the synchronization of the pulses with layer completion. Due to the possible desorption in (B), however, synchronization can be achieved only approximately in this case.

We investigate these different methods by comparing the *surface width*

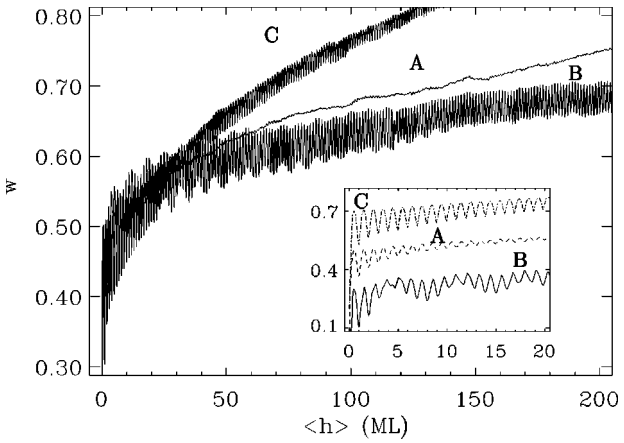

FIG. 4. Comparison of the surface width for conventional growth (*A*) and the flush technique as described in the text. We consider the flush technique with (*B*) and without (*C*) desorption. The inset shows the surface width oscillations during the deposition of the first 20 ML. For clarity of presentation we have shifted the upper (lower) curve about $+0.2\,(-0.2)$ inside the inset. These simulations were carried out on a 512×512 lattice at 560 K. The results are obtained from three independent simulation runs in each case.

$$w=\sqrt{\langle[h(x,y)-\langle h\rangle]^2\rangle}. \tag{3}$$

Perfect layer-by-layer growth would lead to oscillations between zero and 0.5 (coverage of half a monolayer). Higher values of *w* indicate a broader distribution of the heights.

After the deposition of 60 ML using the different techniques the surface widths become considerably different (see Fig. 4). The flush mode without desorption (*C*) is even farther away from perfect layer-by-layer growth compared to conventional growth (*A*). The flush mode in the presence of desorption (*B*) is superior to both (*A*) and (*C*) in the long run, and keeps the surface smooth. Looking at the deposition of the first 20 ML, this seems to be surprising. The oscillations of *w* with technique (*B*) are disrupted due to an obvious asynchronization. With (*C*) the synchronization is perfect leading to very strong and regular oscillations. Using the conventional technique (*A*), the oscillations are damped and much less pronounced.

To summarize, the usage of the proposed flush technique is useful to improve the growth rate (we achieved a factor 2 at high *T*) and to assist layer-by-layer growth. Hereby, the desorption of adatoms is crucial to achieve optimized growth: without desorption the flush mode is worse compared to conventional growth even though strong oscillations are induced. The reevaporation has such an impact because it is *height selective*, i.e., adatoms on top of existing islands desorb easily whereas adatoms beneath islands preferentially are incorporated in the crystal. Clearly, this height-selective behavior is achieved only when a positive Ehrlich-Schwoebel barrier hinders the particles to be incorporated at step edges from above.

We would like to point out that the usage of a chopped flux has been proposed and investigated by Rosenfeld *et al.*[2] in the framework of the *concept of the two mobilities*. However, our findings show that only in the presence of desorption the occurrence of oscillations is indeed coupled to a reduction of the surface roughness. In Ref. 46 the effect of a chopped flux on island distances was investigated. These findings would allow one to optimize even further in that one calculates the minimal flux intensity and the time of the flush needed in order to achieve an increased island density. Here we have chosen a safe high flux without explicit use of the results of Ref. 46.

IV. OPTIMIZING THE STRUCTURE OF MOUNDS IN 3D GROWTH

Quite generally, layer-by-layer growth,[8] as well as step flow is not attainable forever.[47,48] This can be due to, e.g., Ehrlich-Schwoebel barriers[49] which is typically positive.[50] This favors new nucleation events on top of existing islands which leads to 3D growth sooner or later. In order to optimize MBE growth it is thus also interesting to study the growth of 3D structures by computer simulations.

We will start with a brief summary of our findings for 3D growth on the basis of a simplified model of epitaxial growth.[14,15] This will enable us to introduce the basic concepts. After that, we will show how these results can be used in order to improve 3D growth (to be specified below). We will test this strategy with computer simulations of the SOS model of Sec. II.

The most important simplification we introduced in Ref. 14 was an effective description of diffusion and nucleation. Rather than simulate the simultaneous motion of many adatoms, we concentrated on the simulation of individual particles which is a usual technique for simple growth models.[51,52] Parameters of the model are the diffusion length, and in a similar way SED is considered. Even though a similar SED was introduced in Ref. 53, there, as opposed to the present work, no search for kink sites was implemented.

In MBE the typical length of the step-edge diffusion process depends on the temperature and the flux of the arriving particles.[17] On a one-dimensional substrate the theory of island nucleation predicts a typical distance between nucleation centers of the form

$$l_{\mathrm{SED}}\approx\left(\frac{d}{f}\right)^{1/4}, \tag{4}$$

where *d* is the diffusion constant and *f* the flux of arriving particles.[54] If we apply this theory to the lateral or in-plane growth of a pyramid (concentrating on a slice of 1-ML thickness), the flux *f* can be identified with the reduced flux per unit length of the step edge $f=Fl_T$, where l_T stands for the terrace width. Within this context *d* becomes the diffusion constant for diffusion along the step edge. The scaling relation (4) for l_{SED} was obtained under the restriction that two atoms (i.e., $i^*+1=2$) already form a stable nucleus and no desorption occurs. We note that for greater values of i^* the correct theoretical result has been derived recently.[55] However, for the model as described in Sec. II the assumption of $i^*=1$ is reasonable.

When l_{SED} is of the order of the modeled system size (strong SED), the growth is characterized by the formation of square-based pyramids with a well-defined slope. The step edges are oriented along the lattice coordinates, and the surface width was found in Ref. 14 to grow with a power law

$$w\propto h^{\beta}\quad\text{with}\quad\beta\approx0.45, \tag{5}$$

where β is called the growth exponent.[16] Typically, one expresses the scaling behavior in terms of the elapsed time. However, in the context of this paper it is advantageous to use the mean height h instead (as will become clear soon). The typical distance between the pyramids (the correlation length) was found to be proportional to

$$\xi \propto h^{1/z} \quad \text{and} \quad z=\alpha/\beta \approx 2.3 \tag{6}$$

in accordance with the occurrence of slope selection. More formally this means that the ratio of the typical length scales w and ξ remains constant, and hence $\alpha=1$.

The relatively high growth exponent of 0.45 reflects the fact that the coarsening process is SED assisted.[15] Due to the strong SED, material is moved efficiently toward regions with high densities of kink sites, i.e., toward the contact points of pyramids or mounds. For lower values of l_{SED} the coarsening process is purely noise assisted.[56] Hence the structures are merging more slowly.

If the size of the pyramids exceeds l_{SED} the pyramids lose their perfect shape. The structures become round, and step edges will be fringed.[15] It is clear that due to the coarsening, conventional MBE growth is bound to drive itself into this state.

Now we turn to an investigation of how the latter stage in MBE growth can be prevented. The main idea is that in order to prevent the occurrence of rough step edges, one has to require always that $l_{\mathrm{SED}} \approx \xi$. In the following we demonstrate how to fulfill this condition by varying the flux F of arriving particles. Equally well, one could adapt the growth temperature. However, for this a detailed knowledge of the activation energy of d and the temperature dependence of l_T (Ref. 57) is necessary, which is often not available.

Equating expressions (6) and (4), we obtain the height dependence of the flux,

$$F(h)=ch^{-4/z}, \tag{7}$$

where c is an adequate constant. To reformulate this relation in terms of the time, we use $dh/dt=F$ and solve the resulting differential equation, obtaining

$$h(t) \propto t^{-z/(4+z)}. \tag{8}$$

Reinserting this result into Eq. (7), we obtain that the flux should be varied according to

$$F(t) \propto t^{-4/(4+z)} \approx t^{-0.65}, \tag{9}$$

where we inserted $z=2.3$ according to SED-assisted coarsening.[14]

We applied this strategy to the growth of the SOS model of Sec. II at 560 K. Clearly, SED is not a process which is explicitly considered in this model. Typically, atoms with only a single bond to a step edge will detach and diffuse on the terrace. However, the net result will be the same: single-bonded atoms will be moved to places with higher coordination (kink sites). To prevent the inference of reevaporation, we suppressed this process.[58] However, we checked that even with desorption, the strategy is still applicable and useful. The flux was chosen as shown in Fig. 5. We started with a constant flux of 2 ML/s. After the growth of 20 ML we adapted the flux with time t according to $F=F_0/(t/10\mathrm{s})^{0.65}$.

In Fig. 6 we compare the resulting evolution of the surface width w with a simulation with a constant flux $F=1$ ML/s. With our strategy we obtain a higher growth exponent of $\beta \approx 1/2$ compared to conventional growth with $\beta \approx 1/3$. These exponents fit well to $\beta=0.45$ for strong SED (Ref. 14) and $\beta=0.33$ for intermediate values of l_{SED}.[15] However, the result that w grows fast and is described by a high growth exponent under these optimized growth conditions should not be confused with the notion of a fast roughening, self-affine surface. It just means that the structures are merging fast and the mounds are becoming high and wide. This can be seen directly in Fig. 7. After the deposition of 300 ML under constant flux the structures are small, whereas under optimized growth conditions the resulting structures are larger. Note that because of the higher initial flux of 2 ML/s the island density was much higher in the beginning under optimized growth conditions. Nevertheless the SED-assisted coarsening leads to a considerably fewer number of mounds (approximately ten which should be compared to 20 with the conventional growth).

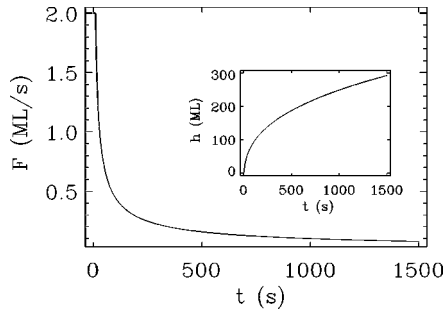

FIG. 5. Flux variation used in the simulation of flux adaption of Fig. 6. The inset shows the reached height in dependence of the time.

It is clear that in order to obtain larger structures in conventional MBE, one just has to grow for longer times. The step edges will become smooth due to the equilibration after the growth has been stopped. However, during growth the

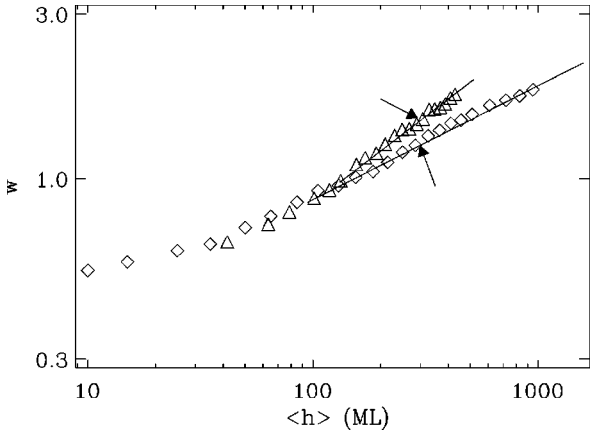

FIG. 6. Comparison of the surface width under optimized growth conditions ($\triangle$) and without an adaption of the flux $F=1$ ML/s ($\diamond$). Under optimized growth conditions the flux was initially set to 2 ML/s, and after 10 s adapted according $F=2/(t/10\mathrm{s})^{0.65}$ ML/s (see Fig. 5). The solid lines correspond to growth exponents $\beta=1/3$ and 1/2. The arrows mark the positions of the snapshots of Fig. 7.

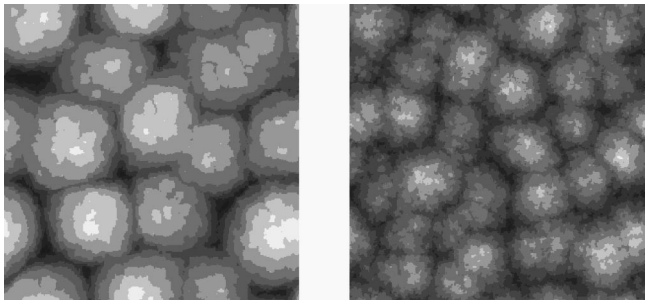

FIG. 7. Snapshots of the surface morphology of 300×300 lattices, where about 300 ML were deposited with two different methods as in Fig. 6 (left: flux adaption; right: conventional growth).

step edges do not remain smooth as in our optimized growth mode. Hence a larger probability for the creation of vacancies or other crystal faults will be present. After growth stops these faults can probably be only partially eliminated in the nonoptimized growth. We also mention that in the end another process will of course become important too. In the limit of $t\rightarrow\infty$ no net growth will be achieved in the optimized growth, and the equilibration of the surface will be dominant.

V. CONCLUSION

We have investigated the effect of the microscopic dynamics on experimentally accessible macroscopic effects in MBE growth. Based on simulations of the solid-on-solid model we proposed two optimized growth strategies.

Comparing the layer-by-layer growth with sublimation, we understood how the desorption of single adatoms comes into play during growth. During growth, freely diffusing adatoms are created by the external flux. During sublimation, however, such adatoms must first be created, e.g., through detachment from steps. This difference manifests itself in the different contributions of the microscopic activation energies to the effective energies. The diffusion barrier E_B increases the effective energy of sublimation, whereas it decreases the activation energy of the desorption rate during growth. Since the macroscopic desorption rate is influenced by the typical lifetime of single atoms, we are able to intervene in the growth process. We showed that a flush mode is able to prolong the layer-by-layer growth regime and to reduce the desorption rate: applying short pulses of particles we create a high density of islands. Afterwards, with a low flux, one completes the monolayer. At least for our particular simulations, the desorption was crucial to obtain improved growth. Even though the flush mode always induces strong oscillations, only in combination with desorption does it lead to an improved growth. This can be explained with the height-selective behavior of desorption, i.e., desorption occurs preferentially on top of islands as long as a positive Ehrlich-Schwoebel barrier is present.

In experiments one should be able to produce such short flushes using a chopper or pulsed-laser deposition in conjunction with conventional MBE. The method should be very useful in order to grow planar coherent thin films, e.g., for application in quantum-well structures. In addition, such experiments would allow one to decide whether desorption occurs out of a physisorbed precursor which has been debated in the literature.[25,42] If so, one should not obtain an improved growth rate using the flush mode.

However, since layer-by-layer growth is unstable, the optimization of 3D growth might be useful too. Based on recent results concerning step-edge diffusion, we proposed varying the flux of arriving particles in order to maintain smooth edges during growth. Reducing the flux according to $F\propto t^{-0.65}$, we were able to recover the high growth exponent of $\beta\approx0.45$ measured on the simplified MBE model.[14] The fast coarsening process (since it is SED assisted) yields structures which soon become very large compared to those of conventional MBE. Irrespective of the desired size of the structures they can be produced under the same (strong SED) conditions, which is accomplished by variation of F. Otherwise the MBE growth would drive itself in the regime where l_{SED} is less than the typical extension of the structures. Thus our method opens additional possibilities for the controlled creation of these self-organized nanostructures by MBE. In addition, this strategy should reduce the probability for the creation of vacancies, since during the conventional growth the rough edges would be overgrown later. However, this is speculative, and cannot be verified in the framework of the solid-on-solid model.

Typically, rather low fluxes are used in order to improve the quality of the grown structures. However, our result suggests that it is not disadvantageous to apply higher fluxes in the beginning. In the end, when the resulting structures are rather large, it becomes important to reduce the flux in order to adapt it to the *smoothing range* of the step-edge diffusion.

ACKNOWLEDGMENTS

This work was supported by the Deutsche Forschungsgemeinschaft through Sonderforschungsbereich 410.

*Author to whom correspondence should be addressed. FAX:+49-931-888-4604. Electronic address: schinzer@physik.uni-wuerzburg.de

[1] M. A. Hermann and H. Sitter, *Molecular Beam Epitaxy* (Springer, Berlin, 1996), 2nd revised and updated edition.

[2] G. Rosenfeld, N.N. Lipkin, W. Wulfhekel, J. Kliewer, K. Morgenstern, B. Poelsema, and G. Comsa, Appl. Phys. A: Solids Surf. **61**, 455 (1995).

[3] J. Jacobsen and J.P. Sethna, Surf. Sci. **411**, 858 (1998).

[4] P. Juzza, W. Faschinger, K. Hingerl, and H. Sitter, Semicond. Sci. Technol. **5**, 191 (1990).

[5] S. Oehling, M. Ehinger, W. Spahn, A. Waag, C.R. Becker, and G. Landwehr, J. Appl. Phys. **79**, 748 (1996).

[6] I. Ulmer, N. Magnea, H. Mariette, and P. Gentile, J. Cryst. Growth **111**, 711 (1991).

[7] By *conventional* MBE, we mean the growth under a constant flux at constant temperature, which will be opposed to *unconventional* MBE as the strategies described in this paper.

[8] H. Kallabis, L. Brendel, J. Krug, and D.E. Wolf, Int. J. Mod. Phys. B **11**, 3621 (1997).

[9] H. Kallabis, L. Brendel, P. Šmilauer, J. Krug, and D.E. Wolf, cond-mat/9901178 (unpublished).

[10] P. Jensen, H. Larralde, and A. Pimpinelli, Phys. Rev. B **55**, 2556 (1997).

[11] J.G. Amar and F. Family, Phys. Rev. Lett. **77**, 4584 (1996).
[12] M. Schroeder, P. Šmilauer, and D.E. Wolf, Phys. Rev. B **55**, 10 814 (1997).
[13] S. Schinzer, M. Sokolowski, M. Biehl, and W. Kinzel, cond-mat/9810007 (unpublished).
[14] M. Biehl, W. Kinzel, and S. Schinzer, Europhys. Lett. **41**, 443 (1998).
[15] S. Schinzer, M. Kinne, M. Biehl, and W. Kinzel, cond-mat/9808149 (unpublished).
[16] A.-L. Barabási and H. E. Stanley, *Fractal Concepts in Surface Growth* (Cambridge University Press, Cambridge, 1995).
[17] J. Villain and A. Pimpinelli, *Physique de la Croissance Cristalline* (Éditions Eyrolles, Paris, 1995).
[18] J. D. Weeks, *The Roughening Transition* (Plenum Press, New York, 1980), pp. 293–317.
[19] G.H. Gilmer and P. Bennema, J. Appl. Phys. **43**, 1347 (1972).
[20] A.C. Levi and M. Kotrla, J. Phys.: Condens. Matter **9**, 299 (1997).
[21] J. Krug, Adv. Phys. **46**, 139 (1997).
[22] P. Šmilauer and D.D. Vvedensky, Phys. Rev. B **48**, 17 603 (1993).
[23] P.A. Maksym, Semicond. Sci. Technol. **3**, 594 (1988).
[24] V. Pontikis, in *Diffusion in Materials*, edited by A. L. Laskan (Kluwer, Dordrecht, 1990), pp. 37–54.
[25] T. Behr, T. Litz, A. Waag, and G. Landwehr. J. Cryst. Growth **156**, 206 (1995).
[26] G.L. Kellog, Surf. Sci. Rep. **21**, 1 (1994).
[27] A. Kley and M. Scheffler, in *23rd International Conference on the Physics of Semiconductors*, edited by M. Scheffler and R. Zimmermann (World Scientific, Singapore, 1996), pp. 1031–1034.
[28] T. Ohno, Thin Solid Films **272**, 331 (1996).
[29] C.M. Aldao, Surf. Sci. **366**, 483 (1996).
[30] Y.-W. Mo, J. Kleiner, M.B. Webb, and M.G. Lagally, Phys. Rev. Lett. **66**, 1998 (1991).
[31] A. Zangwill, *Physics at Surfaces* (Cambridge University Press, Cambridge, 1988).
[32] G. Ehrlich and F.G. Hudda, J. Chem. Phys. **44**, 1039 (1966).
[33] R.L. Schwoebel and E.J. Shipsey, J. Appl. Phys. **37**, 3682 (1966).
[34] B. Poelsema, R. Kunkel, N. Nagel, A.F. Becker, G. Rosenfeld, L.K. Verheij, and G. Comsa, Appl. Phys. Lett. **53**, 369 (1991).
[35] J.W. Evans, D.E. Sanders, P.A. Thiel, and A.E. DePristo, Phys. Rev. B **41**, 5410 (1990).
[36] Y. Yue, Y.K. Ho, and Z.Y. Pan, Phys. Rev. B **57**, 6685 (1998).
[37] P. Šmilauer, M.R. Wilby, and D.D. Vvedensky, Phys. Rev. B **47**, 4119 (1993).
[38] S. Schinzer and W. Kinzel, Surf. Sci. **401**, 96 (1998).
[39] H. Neureiter, S. Schinzer, W. Kinzel, S. Tatarenko, and M. Sokolowski (unpublished).
[40] A. Arnoult and J. Cibert, Appl. Phys. Lett. **66**, 2397 (1995).
[41] E.S. Tok, J.H. Neave, F.E. Allegretti, J. Zhang, T.S. Jones, and B.A. Joyce, Surf. Sci. **371**, 277 (1997).
[42] E.S. Tok, J.H. Neave, J. Zhang, B.A. Joyce, and T.S. Jones, Surf. Sci. **374**, 397 (1997).
[43] A. Pimpinelli and P. Peyla, J. Cryst. Growth **183**, 311 (1998).
[44] P. Peyla, A. Pimpinelli, J. Cibert, and S. Tatarenko, J. Cryst. Growth **184/185**, 75 (1998).
[45] The sublimation energy can be derived from the oscillation period, e.g., of the width of the height distribution, or for short, the surface width *w*.
[46] P. Jensen and B. Niemeyer, Surf. Sci. **384**, L823 (1997).
[47] J. Krug and M. Schimschak J. Phys. I **5**, 1065 (1995).
[48] M. Rost, P. Šmilauer, and J. Krug, Surf. Sci. **369**, 393 (1996).
[49] J. Villain, J. Phys. I **1**, 19 (1991).
[50] P. Stoltze, J. Phys.: Condens. Matter **6**, 9495 (1994).
[51] D.E. Wolf and J. Villain, Europhys. Lett. **13**, 389 (1990).
[52] S. Das Sarma and P. Tamborenea, Phys. Rev. Lett. **66**, 325 (1991).
[53] M.C. Bartelt and J.W. Evans, Phys. Rev. Lett. **75**, 4250 (1995).
[54] D. E. Wolf, in *Dynamics of Fluctuating Interfaces and Related Phenomena*, edited by D. Kim, H. Park, and B. Kahng (World Scientific, Singapore, 1997), pp. 173–205.
[55] H. Kallabis, P.L. Krapivsky, and D.E. Wolf, Eur. Phys. J. B **5**, 801 (1998).
[56] Lei-Han Tang, P. Šmilauer, and D.D. Vvedensky, Eur. Phys. J. B **2**, 409 (1998).
[57] S. Schinzer, S. Köhler, and G. Reents, cond-mat/9905134 (unpublished).
[58] P. Šmilauer, M. Rost, and J. Krug, cond-mat/9811016 (unpublished).